



Characterization of Dust Calcium Phosphate Obtained from Baghouse Dust Collector during Drying Process

I. Labtani, K. El-Hami*

University of Sultan Moulay Slimane, Faculty Polydisciplinary of Khouribga, Laboratory of Nanosciences and Modeling, Khouribga, Morocco

Received 15 March 2019,
Revised 8 April 2019,
Accepted 10 April 2019

Keywords

- ✓ Baghouse,
- ✓ Calcium phosphate,
- ✓ Drying process,
- ✓ Characterization.

elhami_k@yahoo.com ;
Phone: +212673638424;

Abstract

Baghouse dust collectors are using in the unit of drying located in Beni-Idir Khouribga Morocco, to remove phosphates particles from dust air drying before its expellation through the smokestacks. This energetic process is accompanied by the generation of particle puffs emitted during pulse jet cleaning of the baghouse phosphate dust collector. A small dust phosphate part penetrates to the inside of the filter bag and causes the clogging depth. During maintenance of baghouse phosphate dust collectors, three samples were collected: untreated calcium phosphate dust, calcium phosphate dust from the outside of filter media and calcium phosphate dust from the inside of filter media which causes clogging depth. Thus, the aim of this study is the chemical characterization of the three samples. The chemical investigation was conducted using: scanning electron microscopy (SEM) coupled with the energy dispersive X-ray spectroscopy (EDS), X-ray diffraction (XRD) and X-ray fluorescence (XFR), Raman spectroscopy and Fourier transform infrared spectroscopy (FTIR). The obtained results suggested that there were differences observed regarding the chemical parameters during the drying process.

1. Introduction

Drying phosphate process technology is considered as a promising option to ensure the humidity level of the phosphate required. The purpose of the drying operation is to reduce the humidity of the phosphate to a value of 2%, this step is due to several economic reasons: Reducing transportation cost; water increases transportation costs, the development of the product; the increase of the humidity up to 1% according to the customer's needs. Nowadays, most technology used in this process to recover the phosphates particles of dust-laden air is baghouse dust collectors. Baghouses have long been the interest of many researchers. Many theoretical and experimental studies on this subject have been carried out. Baghouses, or dust collectors are a form of fabric Filters. They have been used since 1900 in the mining industry to separate aerosol particles from gas flows [1]. Baghouse system are unsuited to operate with a range pressure from 2 to 6 bars, these dust collectors offer very high air cleaning efficiency of greater than 99.9% [2]. The main advantage of this technique is that baghouse can operate at high velocity filtration [3]. The pulse jet cleaning method consists of injecting the compressed air in very short duration. The cleaning action creates a shock wave that flows into the entire length of the filter bag and dislodge the dust cake [4]. Another major advantage of this technique is that this operation can be done "online" which not required the cessation of the filtration process. In addition, optimizing the pulse-jet cleaning energy can lead to extend filter bag lifetimes [2]. The opencast mining in the regions of Gantour (including mines in Benguerir and Youssoufia) and Khouribga mainly cause calcium phosphates dust. Additionally the involvement of calcium phosphate dust from the sterile of calcination and finally in drying units. However, industrial dust phosphates affect the environment and can lead to several serious diseases to humans. It may cause respiratory diseases because of a frequent inhalation by the workers. The operation of filtration consists of an alternating clogging and cleaning times. The pneumatic pulse jet cleaning is the technique widely used for the regeneration of filter media. According to the critical nature of the particles emitted in the phosphate industry, the quality of the air expelled in the workplace must be rigorously controlled. A phosphate dust concentration limits value of 50 mg/Nm³ has been recommended in Morocco for the air in expellation smokestacks of baghouse dust collectors. Choosing the appropriate and most efficient filter media could help reduce dust emission. Hence, the most recent bag filter media dispose of surface treatment such as

Polytetrafluoroethylene (PTFE) membrane and calendaring. Furthermore, the use of treated filter media has a better effect on cleaning [5] and increase filtration efficiency [6]. Despite the use of surface treated filter media, the problem of depth clogging media persists. Depth filtration refers to media that retains finer particles through the thickness. The behavior of dust phosphates particles during filtration is determined by such properties as size and chemical structure properties. In this context, detailed chemical characterization is investigated for the dust phosphate. It is very important to regard how each characteristic is disseminated to understand the effect of particle properties based on in-depth clogging [7].

2. Material and Methods

2.1. Material

The dust phosphate samples used in this study were collected from the baghouse of the drying unit located in Beni-Idir Khouribga city of Morocco. The unit of drying has a capacity of 67 600 Tons/day and it is equipped with an air filtration system consisting of three essential components: Baghouse dust collector, aspiration system and smokestacks. The dust phosphate samples taken from the baghouse were collected as received and transferred to accomplish different laboratory analyses, no sample preparation was performed. Table 1 summarizes the three samples as it has been described in the previous section.

Table 1: The three samples tested

Sample 1	Sample 2	Sample 3
Untreated calcium phosphate dust	Calcium phosphate dust from the outside of filter media	Calcium phosphate dust from the inside of filter media

2.2. Experimental characterization methods

The elementary composition of the three samples was determined by X-ray fluorescence (XRF) using Epsilon 3X PANalytical spectrometer. Crystalline structure in the dust phosphates samples was analyzed by X-ray diffraction (XRD) named D2 PHASER Bruker with CuK α radiation (CuK α 1,541874 Å) with a LYNXEYE detector, each sample was analyzed for a period of 20 m. The identification of the phase was completed by comparing the obtained experimental diagrams with the referenced data of the JCPDS file (Joint committee of powder diffraction standards). The elementary analyses of the samples, as well as their morphology, were determined by the energy dispersive X-ray spectroscopy (EDS) coupled with scanning electron microscopy (SEM) operated in environmental mode type VEGA 3 TESCAN. The functional groups present in the considered samples were performed using the Fourier transform infrared spectroscopy (FTIR) using a vertex 70 DTGS. For this purpose, 0.001 g of powdered dust samples were mixed with 0.099 KBr to form a pellet in a conventional way. Raman spectroscopy analysis of dust samples was run on a DXR 2 Raman microscope.

3. Results and discussion

3.1. SEM analysis

SEM micrographs of the three dust calcium phosphate samples are shown in Figure 1. The samples from the outside and the inside of filter bags, which are dried at 80 °C (Figure 1(b) and 1(c)), were similar in morphology; these two samples are formed by particles of very irregular shapes and dimensions.

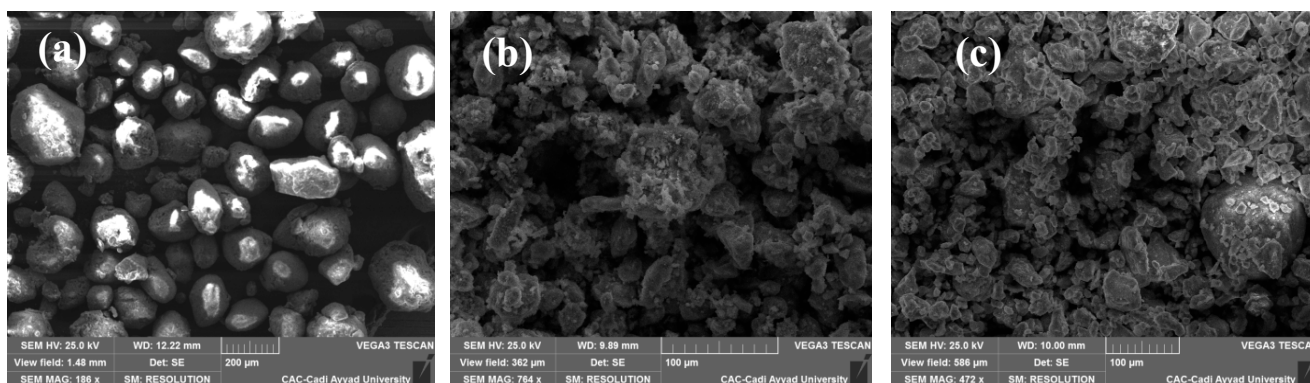


Figure 1: SEM micrographs (a) Untreated dust calcium phosphate (b) dust calcium phosphate from the outside of the filter bag (c) dust calcium phosphate from the inside of the filter bag

The structure of dust powders shows that it is formed by agglomerates with wide range particles size distributions. The size of agglomerates is more important in the dust outside the filter bag compared with the one inside. The SEM micrograph of untreated calcium phosphate is shown in Figure 1 (a). The grains are typically rounded crystals ranging from 33.33 to 266.67 μm . The untreated dust phosphate calcium exhibited a more regular morphology than the two other samples.

3.2 Elemental analysis

Spectra of elemental chemical analysis by EDS technique and FX are summarized in Figure 2 and Figure 3 respectively. As can be seen, EDS analysis showed the same data trend as the XRF analysis, the samples showed the presence of the Ca K peak at about 3.6 KeV for EDS analysis and about 3.7 KeV for XRF analysis. The samples were analyzed by XRF to determine the trace elemental concentrations as shown in Figure 2 and Figure 3.

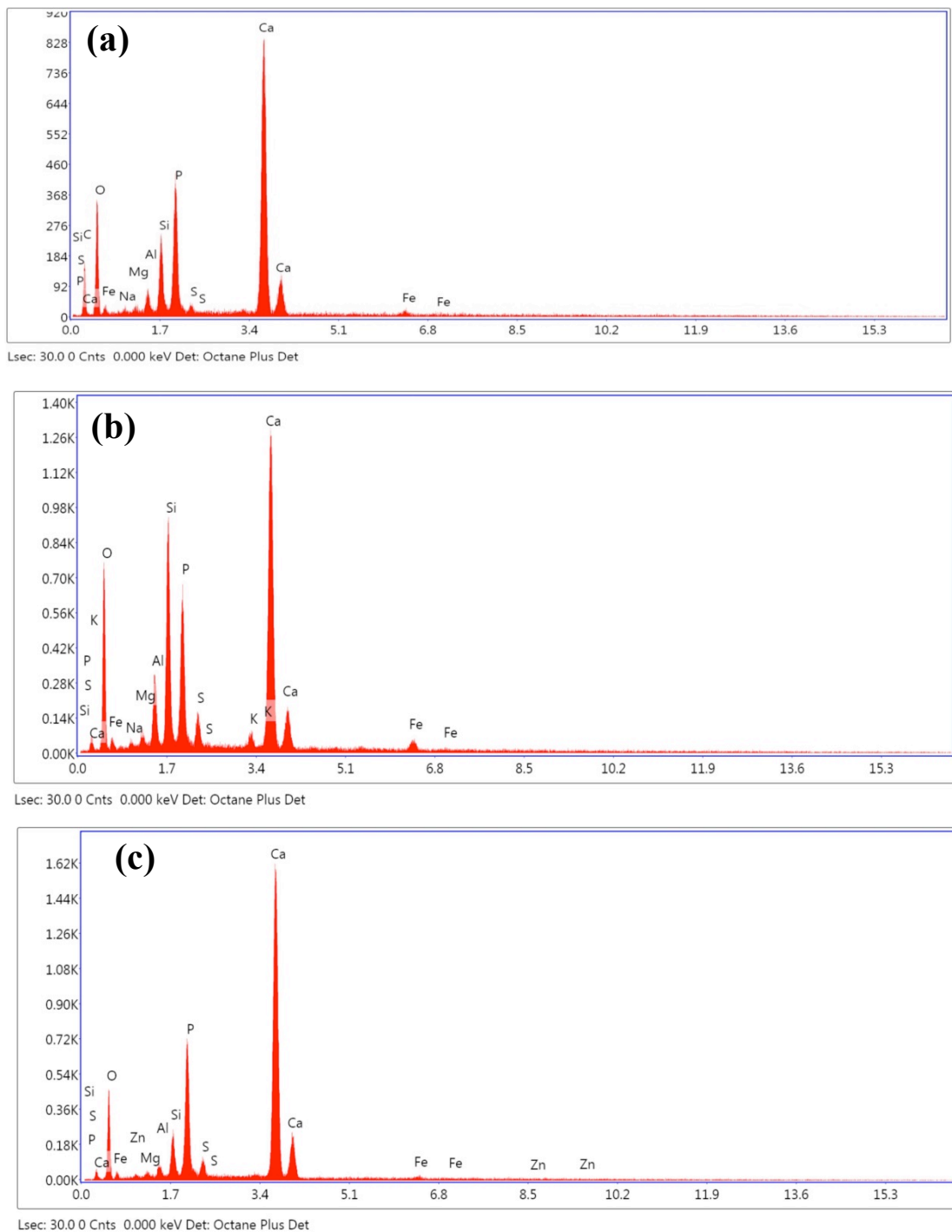


Figure 2: EDS spectra (a) Untreated dust calcium phosphate (b) dust calcium phosphate from the outside of the filter bag (c) dust calcium phosphate from the inside of the filter bag

The XRF spectra revealed additional elements not displayed by EDS. From Figure 2 the major constituents are Ca, P, Si, and O. The minor elements are S, Al, Mg, and Fe. Both major and minor elements, their presence are confirmed by XRF spectra exposed in Figure 3. EDS will not identify low concentration; hence XRF was recorded to distinguish the trace elements. Table 2 summarized the chemical composition obtained from XRF of the three samples. Table 2 studied samples taken from the outside and the inside of filter bags have relatively similar chemical composition relating to the major elements. Small changes in concentration values are observed between the two samples. From the same table, it can be seen that the major element concentration of sample 2 is different from those related to sample 2 and 3.

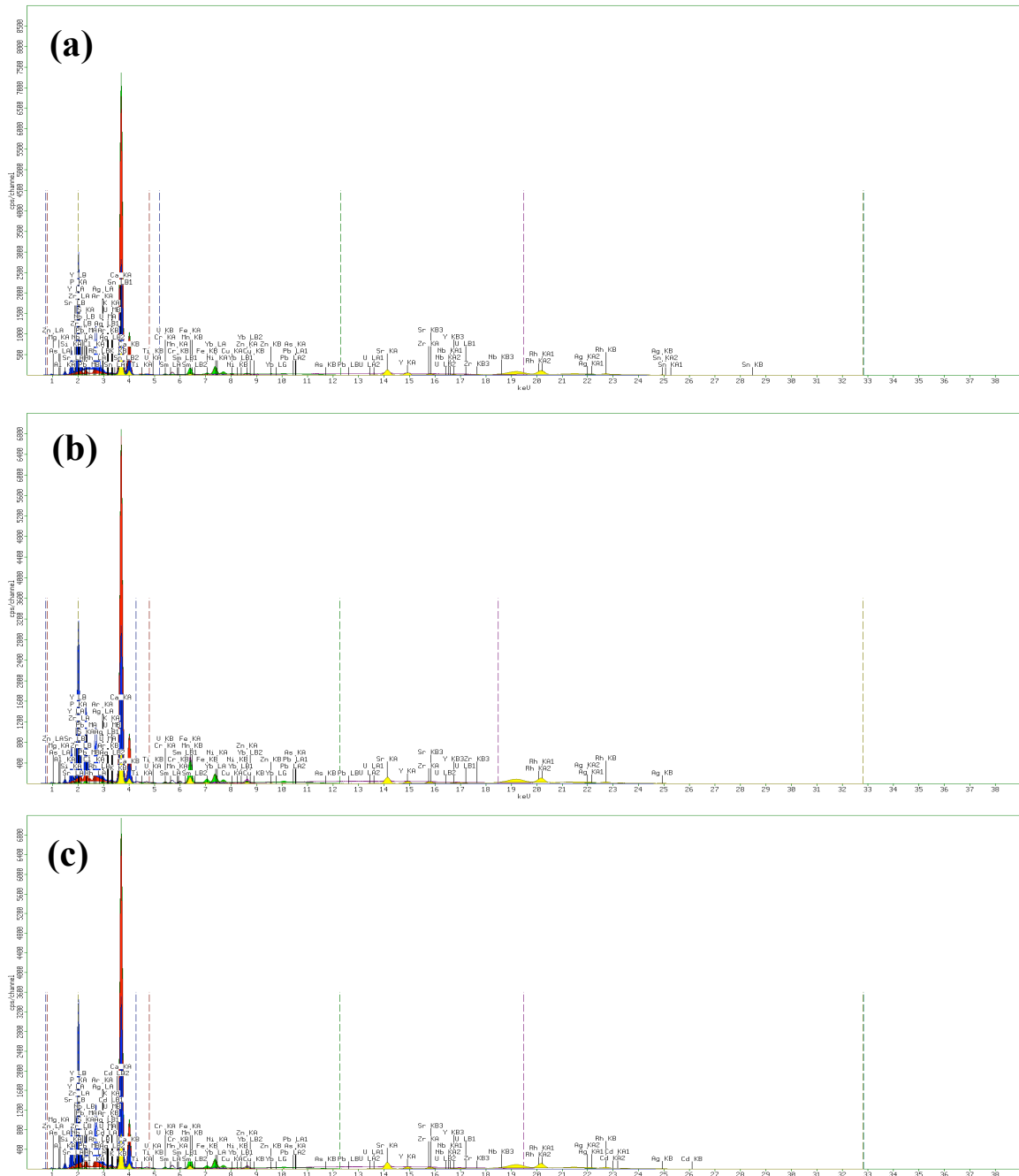


Figure 3: XRF spectra (a) Untreated dust calcium phosphate (b) dust calcium phosphate from the outside of the filter bag (c) dust calcium phosphate from the inside of the filter bag

3.3. X-ray diffraction analysis

X-ray diffraction analysis was examined in order compare the samples regarding their lattice parameters. The structure of natural calcium phosphate is similar to that of Fluorapatite $\text{Ca}_{10}(\text{PO}_4)_3\text{F}_2$, as displayed by X-ray diffraction pattern and chemical analysis in a previous research work [8]. Apatite group minerals including Fluorapatite have a hexagonal crystal structure (P63/m) [9]. Table 3 recapitulates the calculated cell parameters

of the three baghouse samples used in this study. Figure 4 exposed the X-ray diffraction patterns of the three baghouse samples. As can be seen, the peak intensity of the diffraction profiles decreases from samples 3 to 1 indicating that the phosphate from the inside of the bag is well crystallized. This is due to the drying temperature. All the diffraction peaks can be attributed to the Fluorapatite $\text{Ca}_{10}(\text{PO}_4)_3\text{F}_2$ (JCPDS no. 09-0432). Cell parameters and space group found in this study are in agreement with those in the literature, where $a=b=9.368 \text{ \AA}$ and $c=6.884 \text{ \AA}$ [10].

Table 2: Chemical composition of the three baghouse samples

Elements	Samples		
	S1	S2	S3
Ca	33.33%	40.277 %	40.786%
P	5.427%	6.635 %	6.544%
Si	1.450%	2.2017 %	2.286%
Fe	0.429%	1.594 %	0.868%
Al	0.428%	0.456 %	0.565%
S	0.211%	2.349 %	0.738%
Sr	0.136%	0.129 %	0.141%
Ag	0.118%	0.111 %	0.119%
Mg	691.3 ppm	0.201 %	0.191%
Cl	287.1 ppm	0.112 %	254.6 ppm
K	984.4 ppm	0.157 %	0.189%
Ti	748.4 ppm	0.141 %	0.124%
V	357.2 ppm	0.111 %	0.105%
Cr	902.2 ppm	-	0.124%
Y	523.5 ppm	365.3 ppm	419.5 ppm
Zn	485.6 ppm	941 ppm	709.5 ppm
U	287.8 ppm	323.4 ppm	361.3 ppm
Cu	112.4 ppm	84.4 ppm	79.9 ppm
Ni	79.6 ppm	207.2 ppm	185.8 ppm
Zr	70.7 ppm	98.4 ppm	107.8 ppm
Mn	56.5 ppm	-	22.4 ppm
Sn	35.7 ppm	-	-
As	34.4 ppm	32.1 ppm	31.7 ppm
Pb	4.0 ppm	6.4 ppm	5.6 ppm
Cd	-	-	39.8 ppm

Table 3: Cell parameters of the three baghouse samples

Parameters	Samples			
	S1	S2	S3	
Space group	P63/m	P63/m	P63/m	
Crystal system	Hexagonal	Hexagonal	Hexagonal	
Cell parameters	α (°)	90	90	90
	β (°)	90	90	90
	γ (°)	120	120	120
	a (Å)	9.518	9.431	9.429
	b (Å)	9.518	9.431	9.429
	c (Å)	6.844	6.842	6.844
Volume (Å ³)	537.083	527.55	527.089	

3.4. FT-IR and RAMAN analysis

FT-IR spectroscopy was investigated in order to confirm the results of elemental analysis and to approve the phase composition determined by XRD. **Erreur ! Nous n'avons pas trouvé la source du renvoi.** shows the transmittance infrared spectra of the three samples in the 4000 to 400 cm^{-1} region. The most intense absorption peak in 1043 cm^{-1} is assigned to the antisymmetric stretching mode of the P-O bond of PO_4^{3-} Group [11] Bending vibration mode of PO_4^{3-} were observed at 606, 573 and 471 cm^{-1} which attributed to $\text{PO}_4^{3-}\nu_2$.

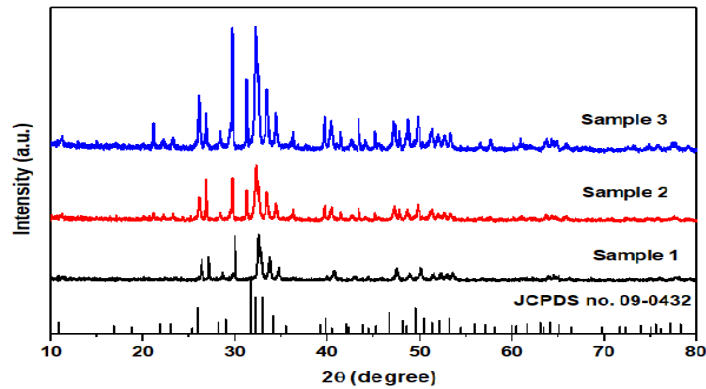


Figure 4. XRD spectra of (sample 1) Untreated dust calcium phosphate (sample 2) dust calcium phosphate from the outside of the filter bag and (sample 3) dust calcium phosphate from the inside of the filter bag

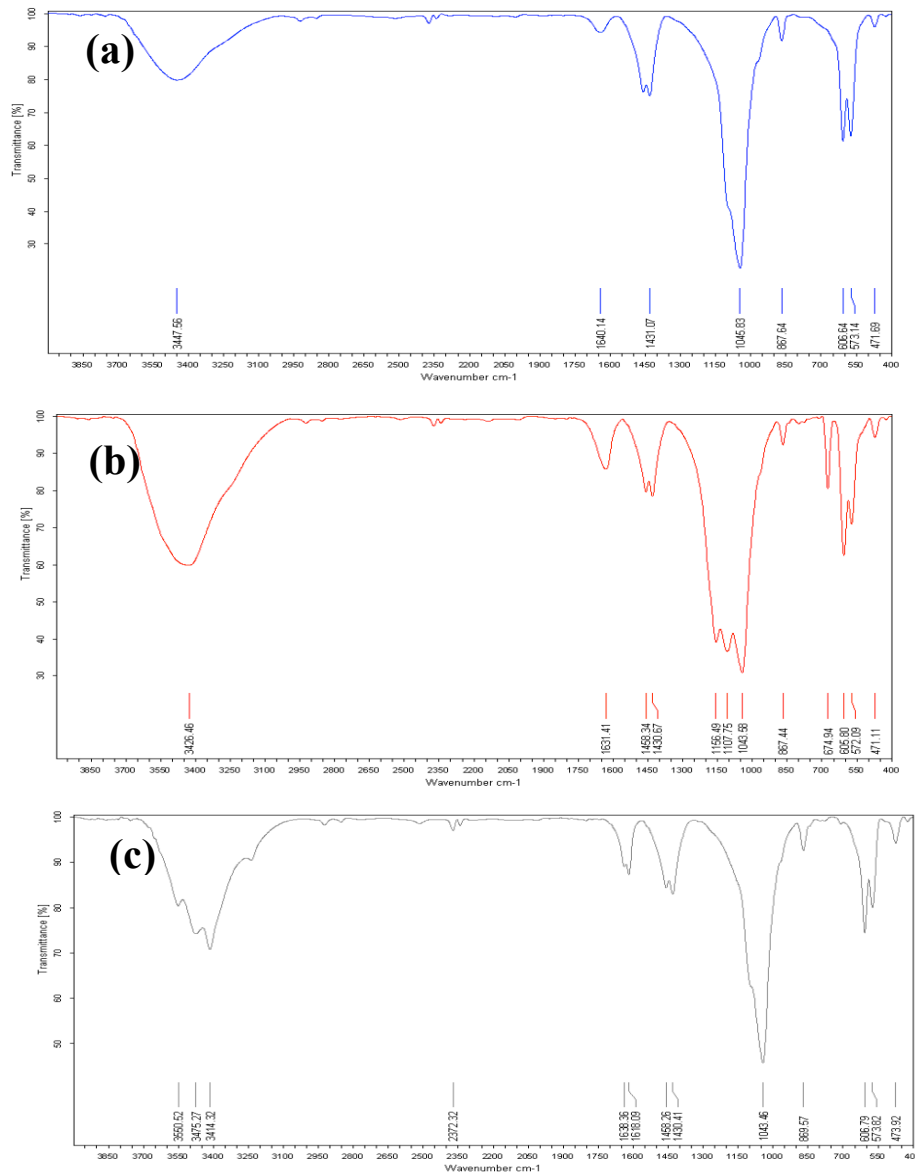


Figure 5: FT-IR spectra (a) Untreated dust calcium phosphate (b) dust calcium phosphate from the outside of the filter bag (c) dust calcium phosphate from the inside of the filter bag

The absorption peaks located at the range from 3400 to 3550 cm^{-1} was derived from the absorbed water and stretching vibrations of structural OH⁻ [12]. The low-intensity band in the region from 1630 to 1640 cm^{-1} is associated with strongly absorbed water [13]. The weak peak around 876 cm^{-1} results from HPO_4^{2-} Vibration [10]. Carbonate vibration at 1430 and 1458 cm^{-1} were present in the samples [14]. FT-IR confirmed the presence of absorbed water and hydroxyl groups, which can be responsible for the formation of agglomerates.

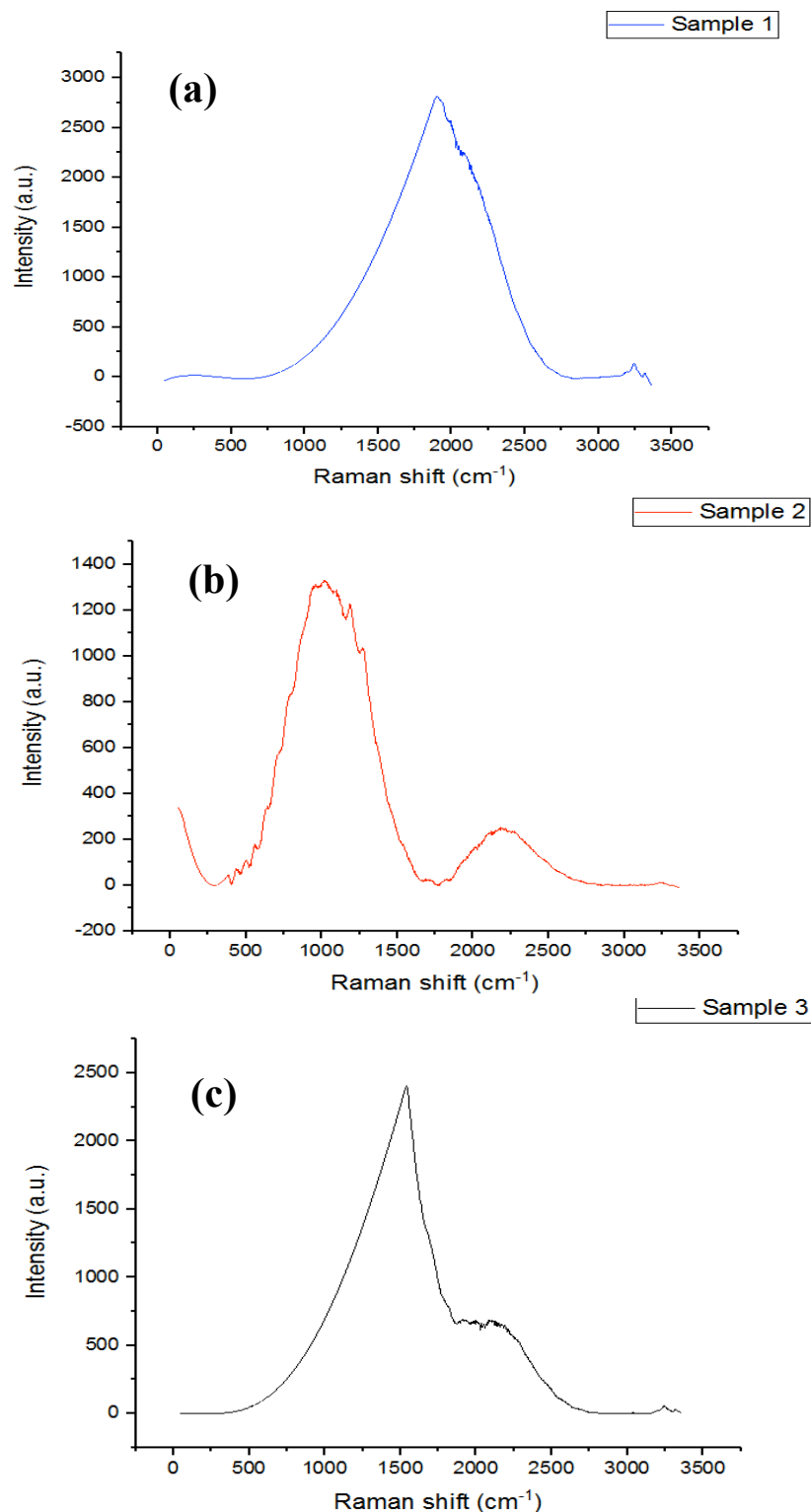


Figure 6: Raman spectra (a) Untreated dust calcium phosphate (b) dust calcium phosphate from the outside of the filter bag (c) dust calcium phosphate from the inside of the filter bag

Raman spectra have been used to differentiate between the three samples through the detection of molecular vibrational mode, and comparing the bands resulting from PO_4^{3-} Modes. The spectra of the three samples over the 0 to 3600 cm^{-1} wave numbers range in the Raman are exposed in **Erreur ! Nous n'avons pas trouvé la source du renvoi.** For sample 1 the spectrum is displayed in Figure 6 (a) as can be seen in one main band is present at around 2003 cm^{-1} which is not assigned. Figure 6 (a) shows the Raman spectrum for sample 2, Raman bands are observed at 946 and 960 cm^{-1} , are assigned to PO_4^{3-} Stretching mode and 994 cm^{-1} are consigned to HPO_4^{2-} . Two antisymmetric stretching bands are detected in 1004 and 1022 cm^{-1} [11,15]. The

Raman spectrum of sample 3 is presented in Figure 6 (c). The intense band at around 1542 cm⁻¹ is attributed to C-H deformation.

Conclusion

In this study, we found and compared the chemical and structural properties of three samples of calcium phosphate being formed in the filters of baghouse dust collectors: untreated dust phosphate, dust phosphate from the outside and that inside the filter bag. However, these dust particles are responsible for the clogging problem and its characterization is an important step in order to find a solution to it. For this purpose, a full set of techniques were applied. SEM analysis showed that the dust phosphate particles from the outside of the filter bag formed more agglomerates that cause clogging depth. Elemental analysis revealed a small change in composition regarding the minor and trace elements. XRD analysis concluded that all the dust phosphate samples are in the hexagonal system (P63/m space group). The vibratory analysis; FT-IR and Raman spectroscopy showed the molecular vibrations and all bands observed referred to the specific phosphates modes. This finding may highlight and indicates both the type of binding of a compound and its crystalline structure.

References

1. N. P. Cheremisinoff, Handbook of chemical processing equipment. Boston: Butterworth-Heinemann, (2000).
2. J. Litchwark, 'Baghouse Design for Milk Powder Collection', (2014)262.
3. C. N. Davies, 'The Separation of Airborne Dust and Particles', *Proceedings of the Institution of Mechanical Engineers, Part B: Management and engineering manufacture*, 1(1953)185–213.
4. K. B. Schnelle and C. A. Brown, Air pollution control technology handbook. Boca Raton: CRC Press, ISBN: 0-8493-9588-7 (2002).
5. Y. Qian, Y. Bi, M. Zhang, et al. "Effect of filtration operation and surface treatment on pulse-jet cleaning performance of filter bags," *Powder Technology*, 277(2015)82–8.
6. X. Simon, D. Bémer, S. Chazelet, et al. "Downstream particle puffs emitted during pulse-jet cleaning of a baghouse wood dust collector: Influence of operating conditions and filter surface treatment," *Powder Technology*, 261(2014)61–70.
7. F. Löffler, H. Dietrich, and W. Flatt, "Dust Collection with Bag Filters and Envelope Filters," eBook ISBN 978-3-663-07900-2 (1988).
8. S. Sebti, A. Saber, A. Rhihil, et al. "Claisen–Schmidt condensation catalysis by natural phosphate," *Applied Catalysis A: General*, 206(2001)217–20.
9. P. Comodi, Y. Liu, P. F. Zanazzi, et al. "Structural and vibrational behaviour of fluorapatite with pressure. Part I: in situ single-crystal X-ray diffraction investigation," *Physics and Chemistry of Minerals*, 28 (2001)219–24.
10. M. Wei, J.H Evans, T. Bostrom, et al. "Synthesis and characterization of hydroxyapatite, fluoride-substituted hydroxyapatite and fluorapatite," *Journal of Materials Science: Materials in Medicine*, 14(2003)311–20.
11. R.L. Frost, Y. Xi, R. Scholz, et al. "Vibrational spectroscopic characterization of the phosphate mineral hureaulite – (Mn,Fe)₅(PO₄)₂(HPO₄)₂·4(H₂O)," *Vibrational Spectroscopy*, 66 (2013) 69–75.
12. W. Jastrzębski, M. Sitarz, M. Rokita, et al. "Infrared spectroscopy of different phosphates structures," *Spectrochimica Acta Part A: Molecular and Biomolecular Spectroscopy*, 79(2011)722–7.
13. R.L. Frost, Y. Xi, R. Scholz et al. "Infrared and Raman spectroscopic characterization of the phosphate mineral fairfieldite – Ca₂(Mn²⁺,Fe²⁺)₂(PO₄)₂·2(H₂O)," *Spectrochimica Acta Part A: Molecular and Biomolecular Spectroscopy*, 106(2013)216–23.
14. F. Granados-Correa, J. Bonifacio-Martínez, J. Serrano-Gómez, Synthesis and characterization of calcium phosphate and its relation to Cr(VI) adsorption properties, *Rev. Int. Contam. Ambient.* 26(2010)129-134.
15. P.N. de Aza, F. Guitián, C. Santos, et al. "Vibrational Properties of Calcium Phosphate Compounds. 2. Comparison between Hydroxyapatite and β-Tricalcium Phosphate," *Chemistry of Materials*, 9(1997)916–922

(2018) ; <https://www.jmaterenvironsci.com/>